iJRASET
International Journal For Research in Applied Science and Engineering Technology

INTERNATIONAL JOURNAL FOR RESEARCH

IN APPLIED SCIENCE & ENGINEERING TECHNOLOGY

Volume: 7 **Issue:** IV **Month of publication:** April 2019

DOI: https://doi.org/10.22214/ijraset.2019.4156

www.ijraset.com

Call: 08813907089 | E-mail ID: ijraset@gmail.com

International Journal for Research in Applied Science & Engineering Technology (IJRASET)
ISSN: 2321-9653; IC Value: 45.98; SJ Impact Factor: 6.887
Volume 7 Issue IV, Apr 2019- Available at www.ijraset.com

Structural, Thermal and Magnetic Properties of PMMA-$ZnFe_2O_4$ Nanocomposite Thin Films

Teena James[1], Tomlal Jose E[2], Subin P John[3], Jacob Mathew[4]
[1, 2]*Department of Chemistry, S.B College, Changanacherry, Kerala-686101, India*
[3, 4]*Moss Bauer Research Group, Department of Physics, S.B College, Changanacherry, Kerala-686101, India*

Abstract: ***Spinel zinc ferrite ($ZnFe_2O_4$) was prepared by spray pyrolysis using polymer precursor of zinc nitrate, ferric nitrate and polyvinyl alcohol (PVA). The nanoparticles are then ultrasonically dispersed in PMMA solution and PMMA-$ZnFe_2O_4$ nanocomposite films were prepared by solvent casting method. The $ZnFe_2O_4$ nanoparticles and PMMA-$ZnFe_2O_4$ nanocomposite film were characterized using X-ray diffraction (XRD), Fourier transform infrared spectroscopy (FT-IR), transmission electron microscopy (TEM), thermo gravimetric analysis (TGA) and vibrating sample magnetometer (VSM). Both XRD and FT-IR has confirmed the formation of the nanocomposite and the TEM image revealed that the nanoparticles were well dispersed in the PMMA matrix. The nanocomposite films have thermal stability up to 360^0C as evident from the TG analysis. The VSM measurements done on the composite film supported superparamagnetic nature of PMMA-$ZnFe_2O_4$ nanocomposite film.***
Keywords: ***$ZnFe_2O_4$, PMMA, PMMA-$ZnFe_2O_4$ nanocomposite, trnsmission electron microscope (TEM), super paramagnetism.***

I. INTRODUCTION

Magnetic nanoparticles received great attention currently because of their potential commercial applications in ferro fluids, advanced magnetic materials, catalysts,[1-3] bio-magnetic separation, magnetic biosensing, magnetic resonance imaging (MRI), electronic equipments etc.[4-6] Among various magnetic nanomaterials, transition metal ferrites (MFe_2O_4) became an important group of technological materials because of their properties such as high electrical resistivity, high chemical stability, high saturation magnetization, low eddy current loss, low dielectric loss, ease of preparation, price and performance considerations etc. These properties made them suitable for many applications in magnetic, mechanical, electronic, catalytic and microwave devices. [7-13] Among spinel ferrites, $ZnFe_2O_4$ is the most studied system. The crystalline bulk form of $ZnFe_2O_4$ is a normal spinel in which Zn^{2+} ions occupy the tetrahedral sites (A site) and Fe^{3+} ions occupy the octahedral sites (B site) and is an ordered antiferro magnet below 10K. However the nano crystalline $ZnFe_2O_4$ has partly inverted spinel structure which can be represented by the formula $[Zn_\delta Fe_{1-\delta}]^A [Zn_{1-\delta}Fe_{1+\delta}]^B O_4$ where δ is the inversion parameter and they are ferrimagnetically ordered at high temperature and high magnetic moment.[14] The properties of the ferrite nanoparticles largely depend on their quality, structure and the method of preparation. The particle size, crystallinity and morphology of the powders largely influence the properties of the ferrite material and can be controlled by varying reaction conditions. It has been found that ferrite nanoparticles of similar composition prepared by different methods have different magnetic properties. [14] Also because of their anisotropic dipolar interactions, ferrite nanoparticles tend to aggregate to form non homogeneous clusters which in turn adversely affect their magnetic properties. Thus prevention of agglomeration of the nanoparticles is an important factor in determining the quality of the ferrite nanoparticles. Several methods such as encapsulation of nanoparticles with surfactants, chemical treatments, dispersion in polymer matrices etc. have been employed to avoid the agglomeration of the nanoparticles. [15] Ferrite nanoparticles embedded in polymer matrix offer several other advantages. Ferrite polymer composites improve the frequency range of operations, the power handling capacity and the temperature sensitivity of the ferrite devices. The properties of the nanocomposite depend on the properties of both the constituents, ie; the properties of the ferrite nanoparticles as well as the polymer. [9] The interaction at the polymer-ferrite interface also influences the properties of the composite materials. Polymer-ferrite nanocomposites therefore have specific mechanical properties, good formability, toughness etc. which render them to prepare complex magnetic devices. [16] In the present work, $ZnFe_2O_4$ nanoparticles are prepared by spray pyrolysis method. The PMMA-$ZnFe_2O_4$ nanocomposite suspension is prepared by solvent method in which appropriate quantities of $ZnFe_2O_4$ nanoparticles are dispersed in the PMMA solution by ultrasonication. The resulting solution is then casted on to a clean glass petri dish for the preparation of PMMA-$ZnFe_2O_4$ nanocomposite thin films. The structural investigations of the samples are carried out using XRD, FT-IR and TEM analyses. The thermal stability of the films is determined from TG analysis and the room temperature magnetic properties of the samples are measured in a vibrating sample magnetometer. The films are found to be super paramagnetic in nature under an applied magnetic field.

II. MATERIALS AND METHODS

A. Materials

Poly methyl methacrylate (PMMA) was used as the polymer host, zinc ferrite ($ZnFe_2O_4$) as the magnetic nano filler and tetrahydrofuran (THF) as the solvent. PMMA of average molecular weight 550000 g/mol was purchased from Alfa Aesar and is used as received. THF was purchased from Merck. The zinc ferrite nanoparticles were synthesized by the spray pyrolysis of polymer precursor solution which was prepared by using zinc nitrate (Merck), ferric nitrate (Merck) and poly vinyl alcohol (PVA, Merck) as starting materials.

B. Preparation of zinc Ferrite Nanoparticles

The zinc ferrite nanoparticles were synthesized by spray pyrolysis of polymer precursor solution. To prepare the precursor solution of zinc ferrite, appropriate quantities of zinc nitrate and ferric nitrate were taken into aqueous solution of PVA which prevent the agglomeration of the metal ions there by ensuring homogeneous distribution of metal ions in the solution. Spray pyrolysis of the resulting PVA-metal nitrates viscous solution at 130^0C followed by annealing at 350^0C for 20 minutes produces zinc ferrite nanoparticles.

C. Preparation of PMMA-$ZnFe_2O_4$ Nano Composite thin Films

PMMA-$ZnFe_2O_4$ nanocomposite solution was prepared by solvent method. A 2% solution of PMMA was prepared by dissolving appropriate amount of PMMA in THF and stirred magnetically for several hours at 45^0C in order to get a homogeneous solution. The polymer nanocomposite suspension was then prepared by the dispersion of appropriate quantities of $ZnFe_2O_4$ nanoparticles in to the polymer solution by ultra sonication. This resulted in the homogeneous distribution of the nanoparticles in the polymer matrix. The resulting nanoparticle suspension was then casted on to a clean glass petri dish and is allowed to dry in air for two days to get thin films of polymer nanocomposites. The prepared films were then allowed to dry in an air oven at 55^0C for the complete removal of the solvent.

D. Characterization

X-ray diffraction (XRD) patterns of the samples were collected from a PANalyitical PW 3040/60 Xpert PRO diffractometer with Cu Kα radiation. Fourier transform infrared (FT-IR) spectra of the samples were recorded using a Perkin-Elmer spectrum 400 spectrometer in the range 400-4000 cm^{-1}. The trnsmission electron microscope (TEM) images were taken in a JEOL, JEM-2100 transmission electron microscope. The thermo gravimetric analysis was carried out in a Perkin Elmer STA 6000 TG analyzer with a heating rate of 10^0C per minute. The room temperature magnetic studies were carried out in a vibrating sample magnetometer (VSM) with a maximum magnetic field of 20kOe.

III. RESULTS AND DISCUSSION

A. X-ray Diffraction(XRD)

Fig 1 shows the XRD patterns of PMMA (a), $ZnFe_2O_4$ nanoparticles (b) and PMMA-$ZnFe_2O_4$ nanocomposite (c).

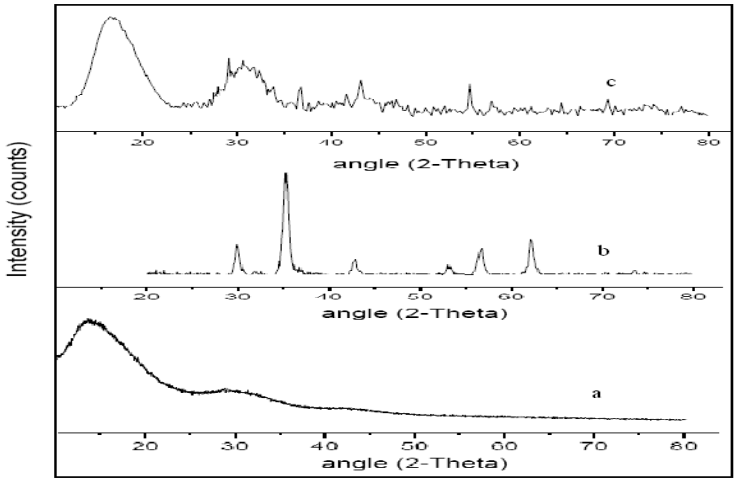

Fig.1. XRD spectra of PMMA (a), zinc ferrite (b) and PMMA-$ZnFe_2O_4$ nanocomposite (c).

XRD pattern of PMMA shows only an amorphous peak between the 2θ values 15^0 and 30^0 as indicated in Fig 1(a). From the diffraction patterns shown in Fig 1(b), confirms cubic spinel structure of the $ZnFe_2O_4$. Using Debye Scherrer formula; $D = 0.9\lambda/\beta\cos\theta$, where D is the crystallite size, λ is the wavelength of Cu Kα, and β is the full width at half maximum (FWHM) and θ is the Bragg's angle; the crystallite size of the particles is found to be around 10nm. Besides the amorphous peak of PMMA; Fig 1(c) shows the characteristic peaks of $ZnFe_2O_4$ nanoparticles; which confirms the formation of PMMA-$ZnFe_2O_4$ nanocomposite. The peaks in Fig 1(c) are less sharp and broadened than the peaks in Fig 1(b). This indicates that the crystallite size of the $ZnFe_2O_4$ nanoparticles decreases as they are introduced to PMMA matrix due to the matrix constraint of the nanoparticles.[17] The crystallite size of the $ZnFe_2O_4$ nanoparticles in the PMMA matrix was determined from TEM pattern and was found to be 7 nm.

B. FT-IR Spectra(FT-IR)

Fig 2 shows the FT-IR spectra of PMMA (a), $ZnFe_2O_4$ nanoparticles (b) and PMMA-$ZnFe_2O_4$ nanocomposite (c). In Fig 2(a), the peak at 2948cm $^{-1}$ is corresponding to C-H stretching vibration; the peak at 1719 cm $^{-1}$ corresponds to the C=O stretching vibration; the peak at 1432cm $^{-1}$ is attributed to the C-H bending vibration; the peak at 1139cm $^{-1}$ is assigned to the C-O-C stretching vibration and peaks between 983cm $^{-1}$ and 749cm $^{-1}$ indicates the bending vibrations of O-C-O bonds of PMMA. Fig 2(b) shows the IR spectrum of $ZnFe_2O_4$ nanoparticles. In ferrites, the metal ions present in octahedral and tetrahedral sub lattices shows different vibrational frequencies. The high frequency band around 600cm $^{-1}$ in the spectrum corresponds to the vibrations of metal ions present in the tetrahedral sites with oxygen atoms. Fig 2(c) also supports the formation of the PMMA-$ZnFe_2O_4$ nanocomposite as the IR spectrum of the nanocomposite contains the characteristic peaks for $ZnFe_2O_4$ nanoparticles along with the peaks corresponding to PMMA. This also indicates that $ZnFe_2O_4$ nanoparticles are well dispersed in the polymer matrix.

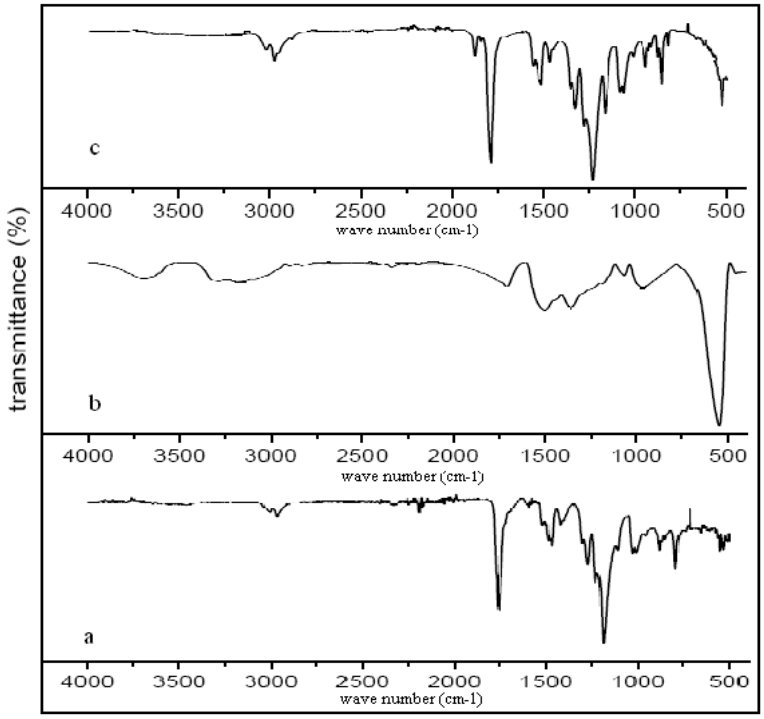

Fig. 2: FT-IR spectra of (a) PMMA, (b) $ZnFe_2O_4$ nanoparticles and (c) PMMA-$ZnFe_2O_4$ nano composite.

C. Morphological Studies

The morphology and particle size of $ZnFe_2O_4$ nanoparticles and PMMA-$ZnFe_2O_4$ nanocomposite film were studied by TEM analysis. Fig 3a shows the TEM image of the $ZnFe_2O_4$ nanoparticles. The TEM image of the $ZnFe_2O_4$ nanoparticles revealed that the particles are agglomerated to a greater extent. This is attributed to the magnetic dipole interactions between the particles. Also the average crystallite size of the particles is found to be around 10 nm, which is consistent with the result obtained from the XRD data. Fig 3b shows the TEM image of PMMA-$ZnFe_2O_4$ nanocomposite thin film. From the TEM image, the nanoparticles are found to be well dispersed in the polymer matrix with an average crystallite size of 7 nm.

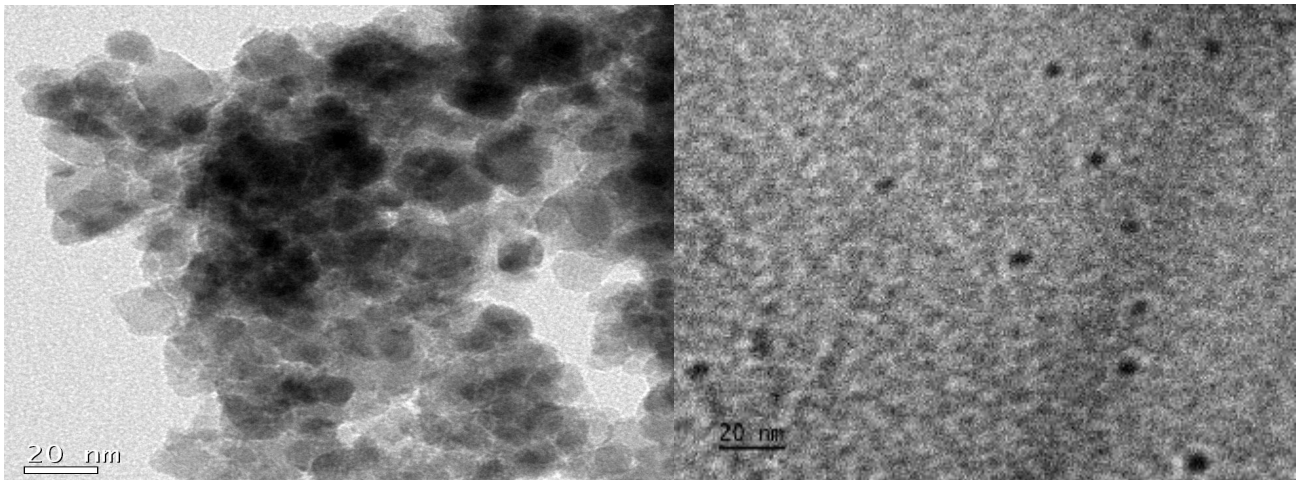

Fig. 3: TEM images of (a) $ZnFe_2O_4$ nanoparticles and (b) PMMA-$ZnFe_2O_4$ nanocomposite film.

D. Thermal Studies

Fig 4 shows the thermo gravimetric (TG) plots for PMMA (a) and PMMA-$ZnFe_2O_4$ nanocomposites (b). The initial weight loss up to 120 ^{0}C is due to the loss of residual solvent and water molecules adsorbed on the film surface. PMMA shows three stages of thermal degradation as evident from the Fig 4a. The first stage of degradation is initiated by scission of weak peroxide and hydro peroxide linkages mainly due to the combination of the monomer with oxygen during synthesis. Head to head linkages formed by termination by combination are also easily broken at lower temperatures, leading to the production of free radicals which will then participate in the further de polymerization at higher temperatures. This first stage, occurs at about 200 ^{0}C, is relatively insignificant as there are a few above mentioned linkages. The second stage at about 300 ^{0}C arises as a result of radical transfer to unsaturated chain ends while the last stage around 365 ^{0}C corresponds to a random scission. From the TGA plots it is clear that the PMMA-$ZnFe_2O_4$ nanocomposite films are thermally stable up to 360 ^{0}C.

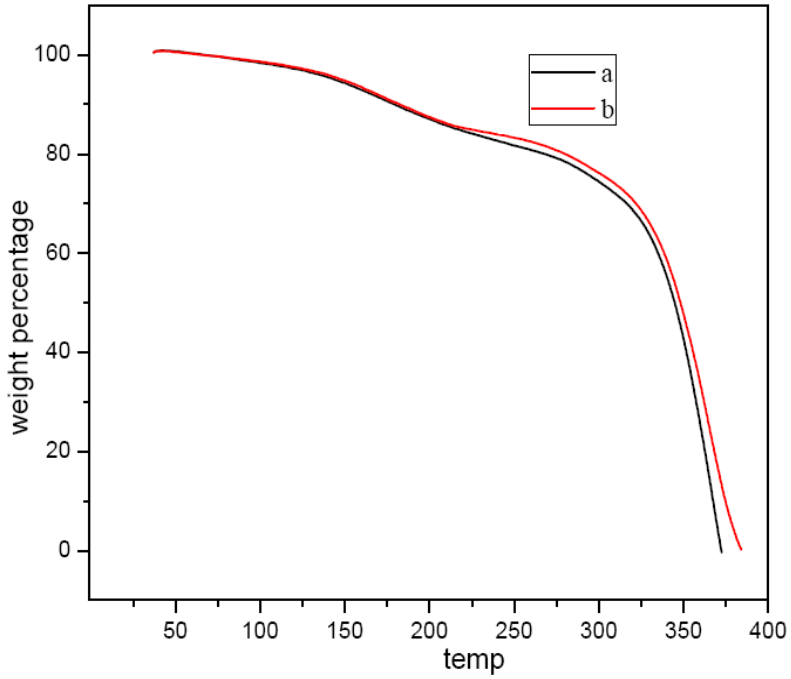

Fig.4. TGA plots for (a) PMMA and (b) PMMA-$ZnFe_2O_4$ nanocomposite film.

E. Magnetic Studies

Fig 5 shows the M-H curves of the as prepared zinc ferrite nanoparticles and PMMA-$ZnFe_2O_4$ nano composite film. PMMA is a non magnetic polymer. [18] From the M-H curve of $ZnFe_2O_4$ nanoparticles, it is clear that the maximum magnetic field of 20 kOe is not enough to saturate the sample. However the samples do not show any hysteresis loop and is paramagnetic in the high field region. The non saturation of the magnetism arises due to the non-homogeneity in the particle size and also due to the agglomeration of the particles. The nanocomposite films of PMMA - $ZnFe_2O_4$ exhibits a clear super paramagnetic behavior since M-H curve shows anhysterectic loop feature and zero magnetic remanance (when H is zero) . This indicates that the size of the particle in PMMA matrix is smaller than the super paramagnetic critical size i.e., the agglomerated nanoparticles are uniformly dispersed in the polymer matrix and thereby reducing the effective size of the particles. Table 1 shows the values of saturation magnetization and magnetic moment of the as prepared $ZnFe_2O_4$ nanoparticles and PMMA-$ZnFe_2O_4$ nanocomposite thin film. An increase in the saturation magnetization (Ms) value of PMMA-$ZnFe_2O_4$ nanocomposite may be attributed to fine dispersion of nanoparticles in the PMMA matrix. This kind of uniform dispersion in polymer matrix inhibits aggregation thereby enhancing magnetic contribution of individual particles to total magnetization of the material.

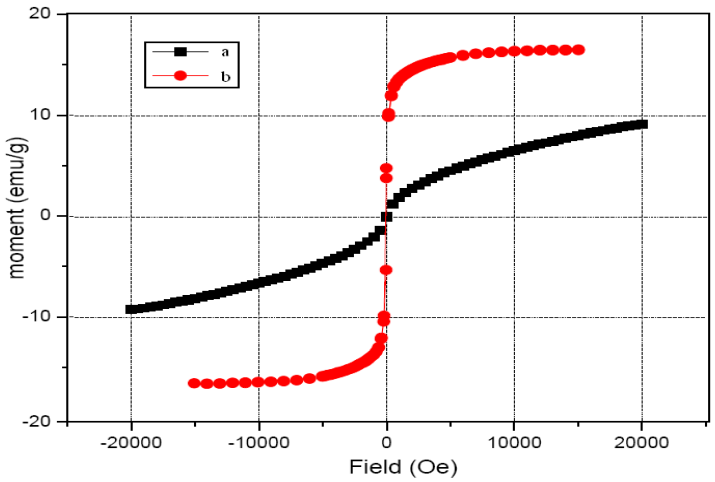

Fig. 5: VSM plots for(a) $ZnFe_2O_4$ nanoparticles and (b) PMMA-$ZnFe_2O_4$ nanocomposite thin film.

TABLE I
Magnetic parameters of $znfe_2o_4$ nanoparticles and pmma-$znfe_2o_4$ nanocomposite.

Sample	Saturation Magnetization (Ms)	Magnetic Moment (μ)
$ZnFe_2O_4$	9.14337	0.39468
PMMA-$ZnFe_2O_4$	16.554	0.71456

IV. CONCLUSION

$ZnFe_2O_4$ nanoparticles are prepared by spray pyrolysis method and are characterized using XRD and FT-IR spectral analyses. The structure of the nanoparticles is confirmed as spinel structure. The average particle size of the nanoparticles is found to be 10 nm. The dispersion of the nanoparticles in PMMA solution by ultrasonication followed by solvent casting of the resulting solution fabricated PMMA-$ZnFe_2O_4$ nanocomposite films. The formation of the nanocomposite was confirmed from both XRD and FT-IR spectra and the average particle size of the nanoparticles is found to be decreased when incorporated in the polymer matrix. The TEM image reveals that incorporation of $ZnFe_2O_4$ nanoparticles in to the PMMA matrix prevents the nanoparticles from agglomeration and as a result, the nanocomposite exhibits a clear super paramagnetic behavior at room temperature which was absent in the M-H curve of $ZnFe_2O_4$ nanoparticles due to the agglomeration of the nanoparticles. Also, the nanocomposite films are found to be stable up to 360^0C.

V. ACKNOWLEDGEMENT

The authors would like to thank the University Grants Commission (UGC) for their financial support.

REFERENCES

[1] F. Caruso, M. Spasova, A. Susha, M. Giersig, R. A. Crauso, (2001) Chemistry of Materials Vol.13 pp.109-116
[2] Y. Xiong, X. Xie, S. Chen, Z. Li, (2003) Chemistry- A European Journal Vol. 9 pp.4991-4996
[3] K. Woo, H. J. Lee, J. Ahn, Y. S. Park, (2003) Advanced Materials Vol. 15 pp. 1761-1764
[4] I. Safarik, M. Safarikova, (2004) Biomagnetic Research and Technology Vol. 2 issue. 7
[5] M. Megens, M. J. Prins, (2005) Journal of Magnetism and Magnetic Materials, Vol. 293 pp. 702
[6] D. L. Graham, H. A. Ferreira, P. P. Freitas, (2004) Trends in Biotechnology, Vol. 22 pp. 455
[7] E. Schloeman, (2009) Journal of Magnetism and Magnetic Materials, Vol. 209 pp. 15
[8] M. Pardavi-Horvath, (2000) Journal of Magnetism and Magnetic Materials, Vol. 171, pp. 215-216
[9] R. Dosoudil, J. Franek, M. Usakova, (2006) Journal of Electrical Engineering, Vol. 57 pp. 142-146
[10] J. Kulikowski, (1984) Journal of Magnetism and Magnetic Materials, Vol. 41 pp. 56
[11] A. P. Alivisatos, (1996) Science Vol. 271(5251), pp. 933-937
[12] M. Sujimoto, (1999) Journal of American Ceramic Society, Vol. 82, Issue:2, pp. 269-280
[13] H.M. Fan, J. B. Yi, (2009) ACS nano, Vol. 3 Issue:9, pp. 2798-2808
[14] M. Thomas, K. C. George, (2009) Indian Journal of Pure and Applied Physics, Vol. 47 pp. 81-86
[15] L. Li, H. Liu, Y. Wang, J. Jiang, F. Xu, (2008) Journal of Colloid and Interface Science, Vol. 32, pp. 265-271
[16] L. Valko, P. Bucek, R. Dosoudil, M. Usakova, (2003) Electrical Engineering, Vol. 54, Issues: 3, pp. 100-103
[17] S. Liu, X. Wei, M. Chu, J.Peng, Y. Xu, , (2006) Colloids and Surfaces B, Vol.51, pp.101
[18] J. Jiang, (2007) European Polymer Journal, Vol. 43, pp. 1724-1728

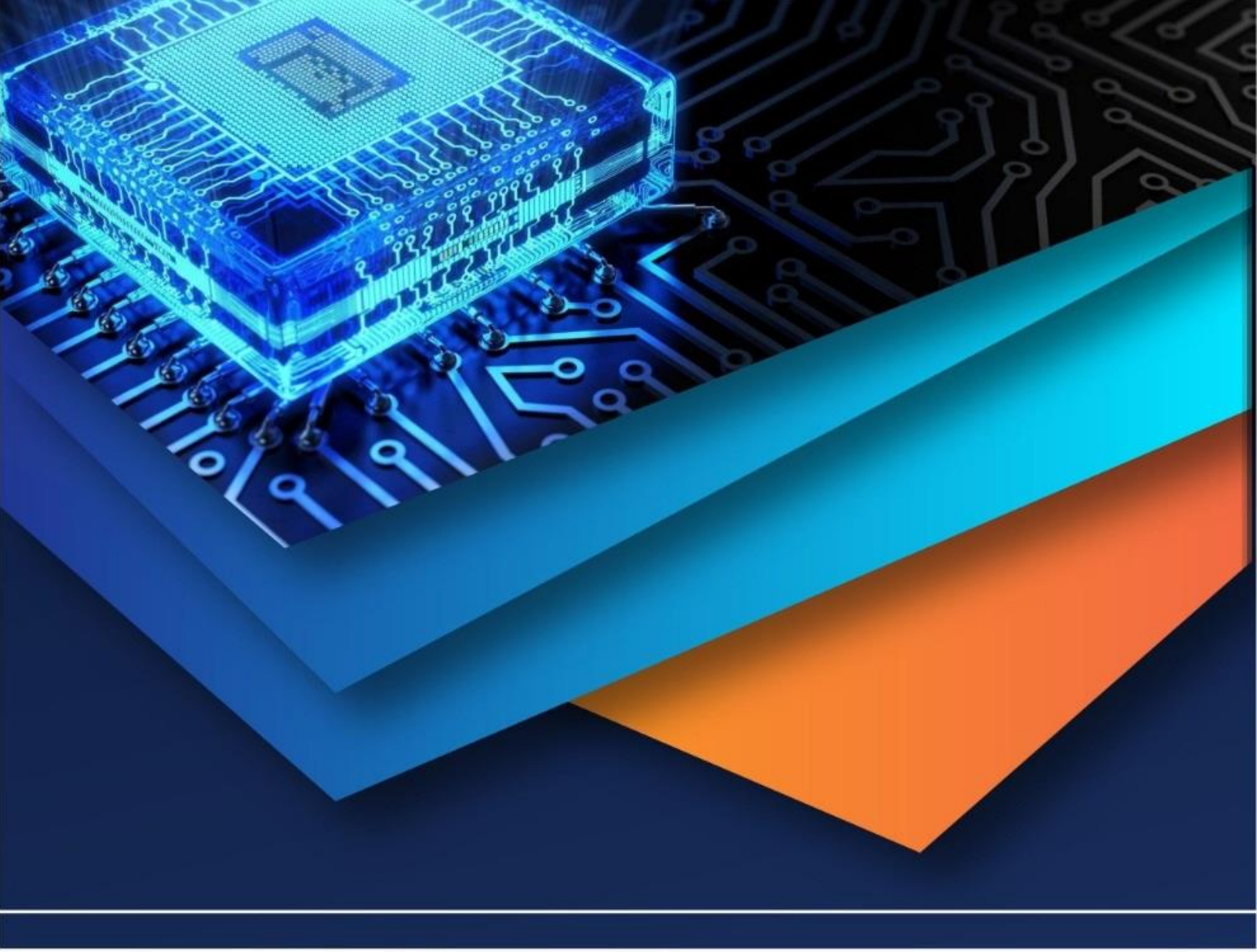

10.22214/IJRASET

45.98

IMPACT FACTOR: 7.129

IMPACT FACTOR: 7.429

INTERNATIONAL JOURNAL FOR RESEARCH

IN APPLIED SCIENCE & ENGINEERING TECHNOLOGY